© 2021. Published by The Company of Biologists Ltd | Development (2021) 148, dev199265. doi:10.1242/dev.199265

RESEARCH REPORT

Single-minded 2 is required for left-right asymmetric stomach morphogenesis

Brent H. Wyatt[1,*], Nirav M. Amin[1,*], Kristen Bagley[1], Dustin J. Wcisel[1], Michael K. Dush[1], Jeffrey A. Yoder[1,2,3] and Nanette M. Nascone-Yoder[1,2,3,‡]

ABSTRACT

The morphogenesis of left-right (LR) asymmetry is a crucial phase of organogenesis. In the digestive tract, the development of anatomical asymmetry is first evident in the leftward curvature of the stomach. To elucidate the molecular events that shape this archetypal laterality, we performed transcriptome analyses of the left versus right sides of the developing stomach in frog embryos. Besides the known LR gene *pitx2*, the only gene found to be expressed asymmetrically throughout all stages of curvature was *single-minded 2* (*sim2*), a Down Syndrome-related transcription factor and homolog of a *Drosophila* gene (*sim*) required for LR asymmetric looping of the fly gut. We demonstrate that *sim2* functions downstream of LR patterning cues to regulate key cellular properties and behaviors in the left stomach epithelium that drive asymmetric curvature. Our results reveal unexpected convergent cooption of single-minded genes during the evolution of LR asymmetric morphogenesis, and have implications for dose-dependent roles of laterality factors in non-laterality-related birth defects.

KEY WORDS: Left-right asymmetry, Stomach, Morphogenesis, Pitx2, Sim2, Down syndrome, Frog

INTRODUCTION

Vertebrate anatomy is characterized by left-right (LR) asymmetries in multiple organs of the cardiovascular, respiratory, digestive and lymphatic systems (Grimes and Burdine, 2017), many of which are derived from or closely associated with, the primitive gut tube (Grzymkowski et al., 2020). Examples of gut tube-derived asymmetries include the differentially lobed left and right lungs, or the disparate proportions of the left and right halves of the liver. However, in most species, the first region of the gut tube to manifest LR asymmetry is the stomach, which curves sharply leftward. The curvature process is driven by asymmetries in cell rearrangement that thin and expand the layers of the left stomach wall (Davis et al., 2017); differential expansion of the contralateral walls of the stomach tube thus impels the organ to curve. Although this process is dependent on global embryonic LR patterning cues, including expression of *Pitx2* on the left side of the foregut (Grzymkowski et al., 2020), the side-specific morphogenetic programs that distinguish the left versus right sides of most asymmetric organs, including the stomach, remain largely unknown. Such knowledge is vital for understanding the evolution of digestive organ morphology and function, as well as for illuminating the etiology of laterality-related birth defects in gut tube-derived tissues in diverse organ systems.

[1]Department of Molecular Biomedical Sciences, North Carolina State University, Raleigh, NC 27607, USA. [2]Center for Human Health and the Environment, North Carolina State University, Raleigh, NC 27607, USA. [3]Comparative Medicine Institute, North Carolina State University, Raleigh, NC 27607, USA.
*These authors contributed equally to this work

[‡]Author for correspondence (nmnascon@ncsu.edu)

N.M.N.-Y., 0000-0003-1301-5298

Handling Editor: Steve Wilson
Received 5 January 2021; Accepted 23 June 2021

RESULTS AND DISCUSSION

sim2 is expressed in the left stomach endoderm

To identify factors likely to drive stomach curvature, we took advantage of Budgett's frog embryos (*Lepidobatrachus laevis*); their extra-large size enables facile bisection of early organs not possible in other vertebrate models (Amin et al., 2015). We performed transcriptome profiling of the left and right halves of the developing stomach at successive phases of morphogenesis: before morphological asymmetry [Gosner stage (GS) 18], and early (GS19), mid- (GS20) and late (GS21) curvature (Fig. 1A; Gosner, 1960).

Differential expression analyses revealed 544 genes with significantly (q-value≤0.05) left or right-enriched expression during at least one phase of curvature morphogenesis (Table S1). The temporal laterality of 278 of these genes (with q-values ≤0.01) is highlighted in Fig. 1B, with more left-enriched (179) than right-enriched (99) genes identified (Fig. 1C). Our list of left-enriched genes includes the transcription factor *pitx2*, which is known to be expressed on the left side of the stomach and other organs (Davis et al., 2017; Grzymkowski et al., 2020). As expected for this master regulator of LR organogenesis, *pitx2* was asymmetrically expressed at all phases of stomach curvature morphogenesis (Fig. 1C,D).

Surprisingly, only one other gene also displayed consistent asymmetric (left-sided) expression across all four stages of curvature (Fig. 1C,D): the highly conserved Per/Arnt/Sim bHLH transcription factor, *single-minded 2* (*sim2*). The prominence of *sim2* in our dataset is noteworthy as this gene is a vertebrate homolog of the *Drosophila single-minded* (*sim*) gene previously found to be required for LR asymmetrical looping of the fly midgut – a structure functionally equivalent to the vertebrate stomach and intestine (Maeda et al., 2007).

Unlike *pitx2*, which is expressed in both inner endodermal (future epithelial lining) and outer mesodermal (future smooth muscle) layers of the left stomach wall (Fig. 1E,F), *sim2* is expressed exclusively in the endoderm layer (Fig. 1G), as revealed by RNA *in situ* hybridization (ISH) in the common laboratory frog, *Xenopus*. The gene is also expressed bilaterally in craniofacial structures (e.g. Fig. S1A-D), pronephric tubules (Fig. S1E), lungs (Fig. S1F) and in a narrow domain of epithelium comprising the dorsal midline of the foregut (asterisks, Fig. 1G and Fig. S1E,F). Below, we describe the functional validation of *sim2* as a new organ-specific regulator of asymmetric morphogenesis. Further analysis of other

Development (2021) 148, dev199265. doi:10.1242/dev.199265

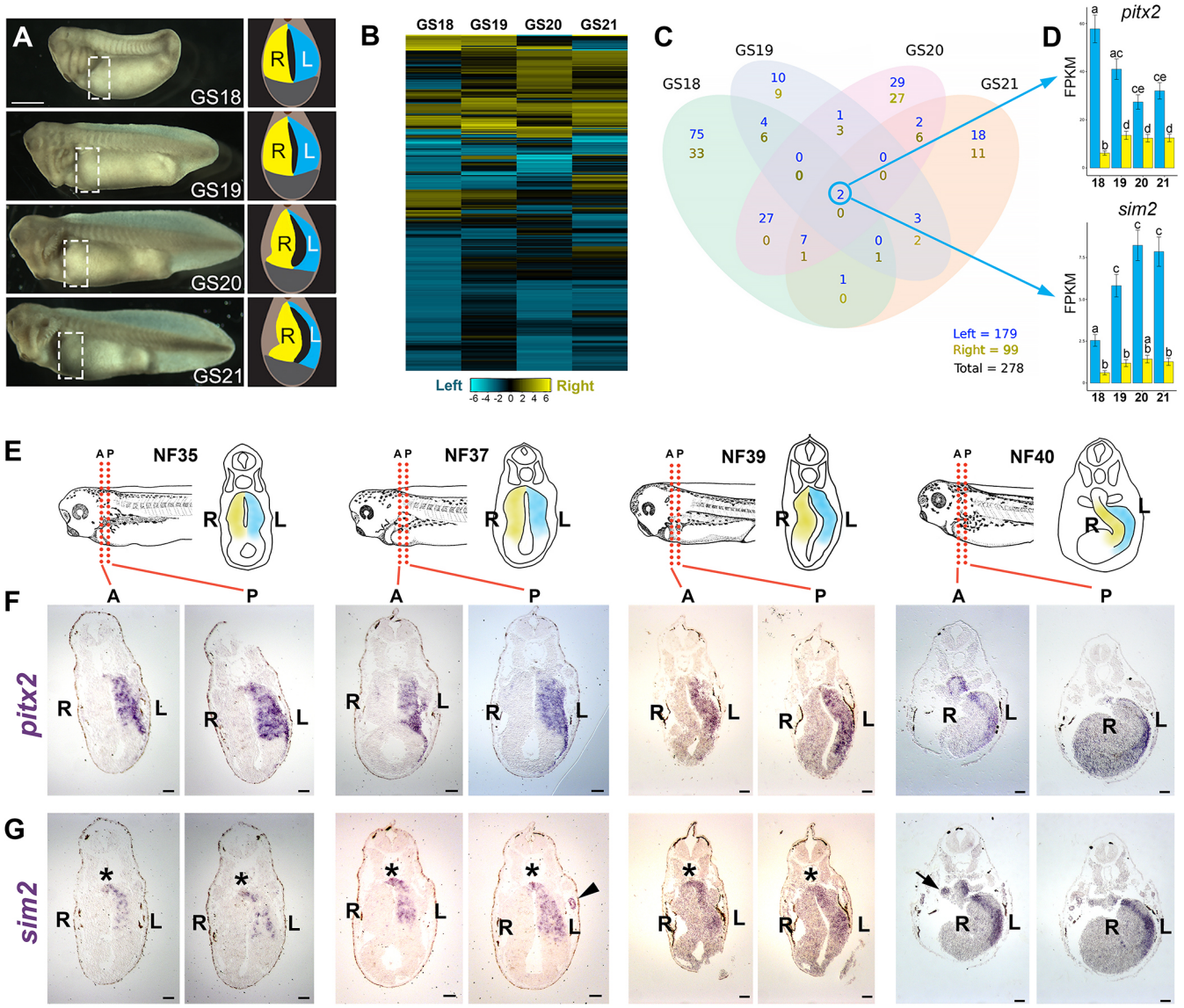

Fig. 1. Left versus right stomach transcriptome analyses identify *sim2*. (A) Left lateral views of *Lepidobatrachus laevis* embryos at stages before (GS18), during (GS19-GS20) and after (GS21) overt stomach curvature; the stomach region is indicated by the white dashed box. Color-coding of transverse sections indicates the left (L; blue) and right (R; yellow) stomach tissues dissected for transcriptome analyses at each phase of curvature. (B) Heat map of 278 *L. laevis* transcripts with significant left (blue; 179) or right (yellow; 99) enrichment at each stage of curvature (q-value≤0.01). (C) Venn diagram showing the number of transcripts with left- or right-enrichment at each stage (q-value≤0.01), as well as those asymmetrically expressed at more than one stage. Although no transcripts are consistently right-sided across all four stages, two transcripts are left-sided throughout stomach curvature: *pitx2* and *sim2*. (D) Left (blue) and right (yellow) expression of *L. laevis pitx2* and *sim2* at each stage of stomach curvature. FPKM, fragments per kilobase of transcript per million mapped reads. Significant differences between sides and stages are indicated by lower case letters, used to label means such that bars bearing different letters are statistically different from one another (P<0.05). (E) Diagrams of *Xenopus* embryos (left lateral and transverse views) at equivalent phases (NF35, NF37, NF39, NF40) of stomach curvature illustrate the approximate planes of section (red dotted lines), and the position of the left (blue) and right (yellow) stomach walls shown in the corresponding tissue sections in F and G. (F,G) The spatial expression patterns of *pitx2* (F) and *sim2* (G) were validated by RNA ISH. Images in G are neighboring sections from the same embryo shown in F; asterisks demarcate expression in the stomach dorsal midline. See Fig. S1 for additional *sim2* expression patterns. Scale bar: 1 mm (A); 500 µm (F,G).

left- and right-enriched genes in our LR transcriptome dataset (Table S1) will be reported elsewhere.

sim2 expression is regulated by LR patterning

To confirm that the left-sided expression of *sim2* is dependent on LR patterning cues, we exposed *Xenopus* embryos to a selective TGF-β receptor inhibitor (SB505124). This compound disrupts the Nodal signaling in the left lateral plate mesoderm (LPM) that is necessary to establish global LR asymmetry (Dush et al., 2011), consequently inhibiting left-sided *pitx2* expression in the left LPM and ultimately leading to random stomach laterality, including straightened and reversed curvatures (Davis et al., 2017).

As expected, the expression of a pan-stomach marker (*sox2*) was unaffected by SB505124 exposure (compare Fig. 2A and D). However, compared with DMSO controls (Fig. 2B), the expression of *pitx2* was reduced or eliminated in stomachs with SB505124-induced straightened or reversed curvatures (Fig. 2E). *sim2* expression in the left stomach wall of SB505124-treated embryos was likewise reduced or eliminated (Fig. 2F) compared with controls (Fig. 2C), paralleling perturbed *pitx2* expression.

Development (2021) 148, dev199265. doi:10.1242/dev.199265

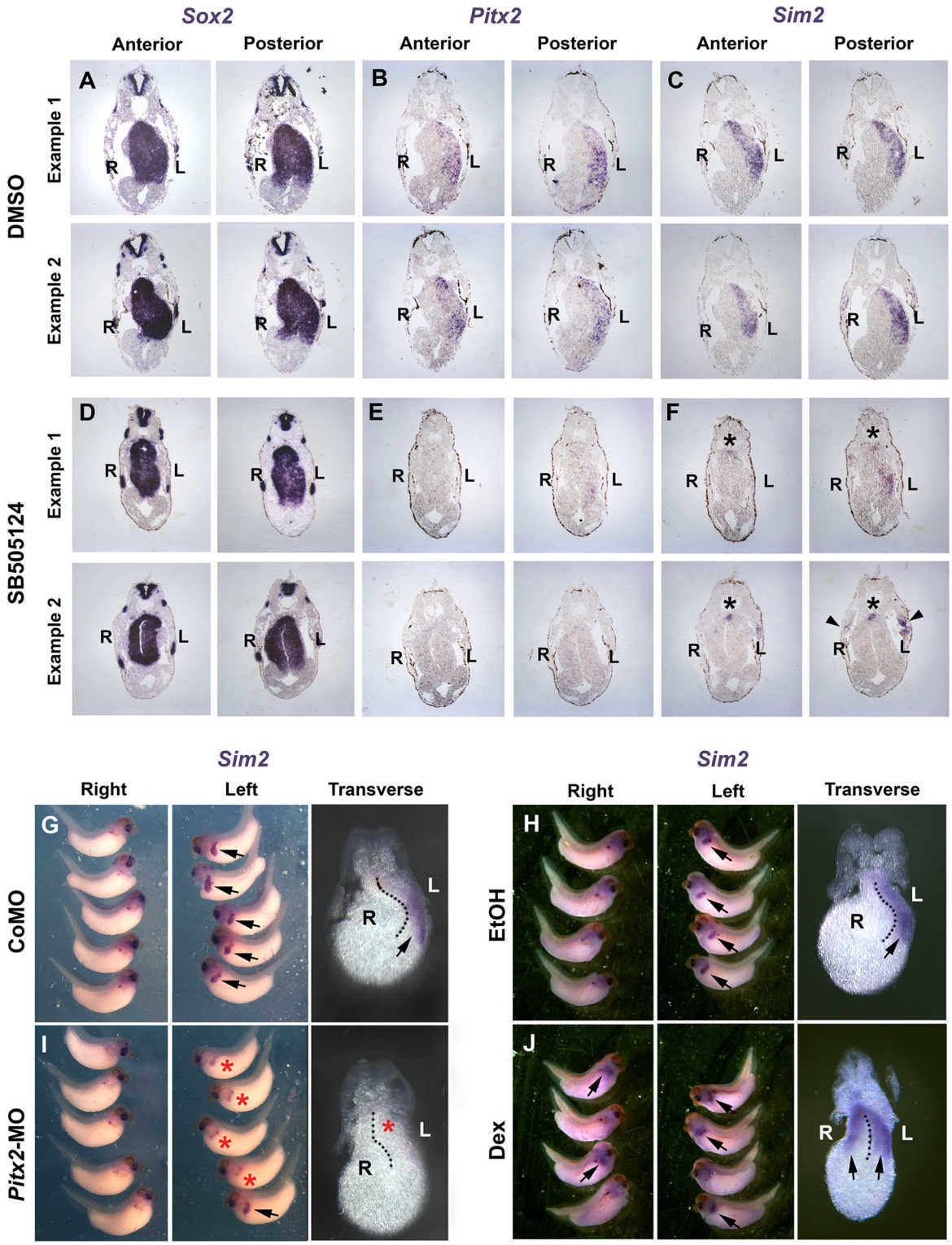

Fig. 2. *Sim2* expression is regulated by LR patterning. (A-F) The expression patterns of *Xenopus sox2* (A,D), *pitx2* (B,E) and *sim2* (C,F) were determined by RNA ISH on anterior and posterior stomach sections from DMSO (A-C; two examples are shown) and two different SB505124-exposed embryos (D-F; NF39) with straightened (Example 1) and reversed (Example 2) stomach curvatures. In A-C and D-F, serial sections from the same individual were hybridized with each probe. Black asterisks and arrowheads in F indicate *sim2* expression retained in the stomach dorsal midline and pronephric tubules, respectively. (G-J) Whole mount RNA ISH with a probe for *sim2* was also performed on embryos injected with either a control (CoMO; G) or *pitx2* morpholino (*pitx2*-MO; I), targeted to the embryo's left side, or injected with mRNA encoding a dexamethasone-inducible *pitx2* construct (*pitx2*-GR) on the right side and exposed to ethanol control (EtOH; H) or dexamethasone (Dex; J). Each embryo in G-J is shown in right and left views, with a representative transverse section through the stomach (NF40) (dotted lines indicate location of lumen). Arrows indicate *sim2* expression evident in the left and/or right stomach walls; red asterisks in I indicate reduction or absence of the expected left side *sim2* expression domains.

Development (2021) 148, dev199265. doi:10.1242/dev.199265

However, the midline (asterisks, Fig. 2F) and bilateral pronephric (arrowheads, Fig. 2F) expression domains of *sim2* remained unaffected by SB505124.

Left-sided *sim2* expression is evident as early as Nieuwkoop and Faber stage (NF) 32 (Nieuwkoop and Faber, 1994) (Fig. S1A,B), shortly after *pitx2* expression is established in the left LPM, and overlaps identically with the endodermal domain of *pitx2* in the left stomach wall (Fig. 1E-G). To test whether *sim2* expression is regulated by Pitx2, we targeted a *pitx2* morpholino (MO) to the left side of the developing stomach, a manipulation that we previously showed knocks down Pitx2 translation and perturbs stomach curvature (Davis et al., 2017). In 94.9% (n=46) of embryos injected with a control-MO, *sim2* expression was left-sided as usual (Fig. 2G). However, *sim2* expression was barely detectable in 66.1% of *pitx2*-MO-injected embryos (n=26; P<0.01; one-way ANOVA; Fig. 2I), suggesting that Pitx2 activity is indeed required for proper expression of *sim2* in the left endoderm.

In the converse experiment, we ectopically expressed Pitx2 on the right side of the stomach by microinjecting mRNA encoding a hormone-inducible version of Pitx2 (*pitx2*-GR; Davis et al., 2017); exposure to dexamethasone was then used to activate ectopic Pitx2 before stomach curvature morphogenesis (Davis et al., 2017). Although aberrant *sim2* expression was rarely seen in ethanol-exposed controls (4.9%; n=65; Fig. 2H), dexamethasone activation of ectopic Pitx2 activity led to expansion and/or bilateral expression of *sim2* on both sides of the stomach in 52.4% of cases (n=71; P<0.01; Fig. 2J). Together, these pharmacological perturbation and epistasis results suggest that Pitx2 is both necessary and sufficient for asymmetrical *sim2* expression.

sim2 is required for cellular events underlying stomach curvature

To determine whether Sim2 is required for proper stomach curvature, we performed CRISPR-mediated editing of the genomic sequence encoding the HLH domain of *sim2* in *Xenopus* embryos (Fig. 3A-H′). Although control F0 embryos (Fig. 3A,C) rarely (5.7%; n=35) exhibited aberrant stomach curvature, 60.1% (n=58; P<0.01) of *sim2* gRNA+Cas9-injected F0 embryos developed straightened stomachs (Fig. 3B,D), correlating with the induction of predicted deleterious indels in the *Xenopus sim2* genomic region (Fig. S2). This result confirms that Sim2 activity is required for proper execution of stomach curvature.

We previously showed that thinning and expansion of the left stomach wall is driven by radial intercalary rearrangement of left endoderm cells, which leads to a significant LR difference in stomach wall thickness (Davis et al., 2017). As *sim2* is expressed in only the endoderm layer of the stomach, we hypothesized that it may play a role in execution of these cell rearrangements. Indeed, the LR difference in stomach wall thickness seen in control embryos (R/L ratio=1.31) was found to be significantly perturbed in *sim2* CRISPants (R/L ratio=0.79; P<0.05). Moreover, in control stomachs, the left wall exhibited layers of radially aligned nuclei that have accumulated near the basement membrane after rearranging (Fig. 3E,G,G′). In contrast, endoderm cells in the straightened *sim2*-CRISPant stomachs remained distributed more broadly and randomly across the width of the left stomach wall, consistent with a failure to undergo the requisite rearrangements (Fig. 3F,H,H′).

To more specifically elucidate the cellular roles of Sim2 in stomach morphogenesis, we localized a *sim2*-MO to the left stomach endoderm (along with GFP mRNA as a lineage tracer for identifying Sim2-deficient cells). Although only 6.6% (n=151) of control-MO injected embryos (Fig. 3I,K,O) had abnormal stomach curvature, 84.5% (n=155) of *sim2*-MO-injected stomachs failed to curve (P<0.01; Fig. 3J,L,P). A second *sim2*-MO had a similar effect (Fig. S3A). This phenotype correlated with translation knockdown (Fig. S3B) and could be partially rescued by co-injection of exogenous MO-resistant *sim2* mRNA (Fig. S3C), confirming the specificity of the result. (Importantly, targeting *sim2*-MO to the right endoderm had no effect on stomach curvature; Fig. S3D.)

As observed in *sim2* CRISPants, the R/L ratio of the width of the stomach epithelium was reduced from 1.51 in controls to 1.01 in *sim2* morphants (P<0.001), indicating failure of the process that normally thins the left wall with respect to the right. Furthermore, whereas control-MO injected endoderm cells formed radially aligned layers in the left stomach wall (Fig. 3M-M″), Sim2-deficient endoderm cells remained randomly distributed (Fig. 3N-N″). As expected for radially intercalating cell populations, endoderm cells injected with control-MO exhibited columnar shapes (Fig. 3M,M′,Q) and parallel arrays of microtubules (MTs) aligned perpendicular to the basement membrane (Fig. 3Q′). In contrast, Sim2-deficient endoderm cells appeared to be round (Fig. 3N,N′,R), with misaligned, randomly-oriented MTs (Fig. 3R′). Importantly, *sim2*-MO injected cells remained proliferative (Fig. S4A,B), suggesting that the abnormal architecture of Sim2-deficient epithelia is not due to decreased viability.

Control cells also displayed robust apicolateral localization of cell-cell adhesion markers, including β-catenin (Fig. 3M′) and E-cadherin (Fig. 3S,S′), as necessary to maintain tissue integrity during epithelial remodeling (Dush and Nascone-Yoder, 2013). In contrast, Sim2-deficient cells exhibited irregularly distributed β-catenin (Fig. 3N′) and E-cadherin (Fig. 3T,T′). These abnormal cell properties were observed at stages before overt curvature (Fig. S4C-J), confirming they precede, and are likely causal to, the stomach morphological defects. Interestingly, β-catenin was sometimes localized to the nucleus in *sim2*-MO-injected cells (Fig. S4H,I), a condition that has been associated with epithelial plasticity (e.g. Kim et al., 2019b); this observation is consistent with previous results suggesting that Sim2 function may be mediated by β-catenin-TCF signaling (Chen et al., 2014). At later stages, GFP-labeled apoptotic cells were occasionally found in the lumen of *sim2*-MO injected stomachs (asterisks, Fig. 3R,R′), suggesting the changes in Sim2-deficient cell properties had rendered them unable to intercalate and ultimately excluded them from the epithelial layer. All cellular phenotypes were rescuable by co-injection of exogenous MO-resistant *sim2* mRNA (Fig. S4K-V), confirming that these effects are specific to Sim2 function. Taken together, our results indicate that Sim2 acts in the left stomach endoderm to govern the properties necessary for cells to radially rearrange and expand the left wall during curvature.

This study comprises the first genome-wide profiling of the left versus right halves of a developing organ as it acquires morphological LR asymmetry, revealing *sim2* as a new LR gene. Our results reveal that, as in flies, single-minded genes also orchestrate asymmetric digestive organ morphogenesis in frogs, suggesting an intriguing cooptive convergence in this bHLH/PAS gene function in insect and amphibian lineages.

In both the fly and frog, *sim/sim2* expression is confined to the epithelial layer of the gut tube, and our findings are consistent with the known roles of single-minded genes in regulating epithelial plasticity in other contexts. For example, in *Drosophila*, *sim* controls the delamination of neuroectoderm cells (Bossing and Technau, 1994; Thomas et al., 1988) and in the mammary epithelium, *Sim2s* (a short isoform) regulates duct and gland formation (Laffin et al., 2008). As in the stomach, *Sim2s* deficiency in the mammary epithelium perturbs

Development (2021) 148, dev199265. doi:10.1242/dev.199265

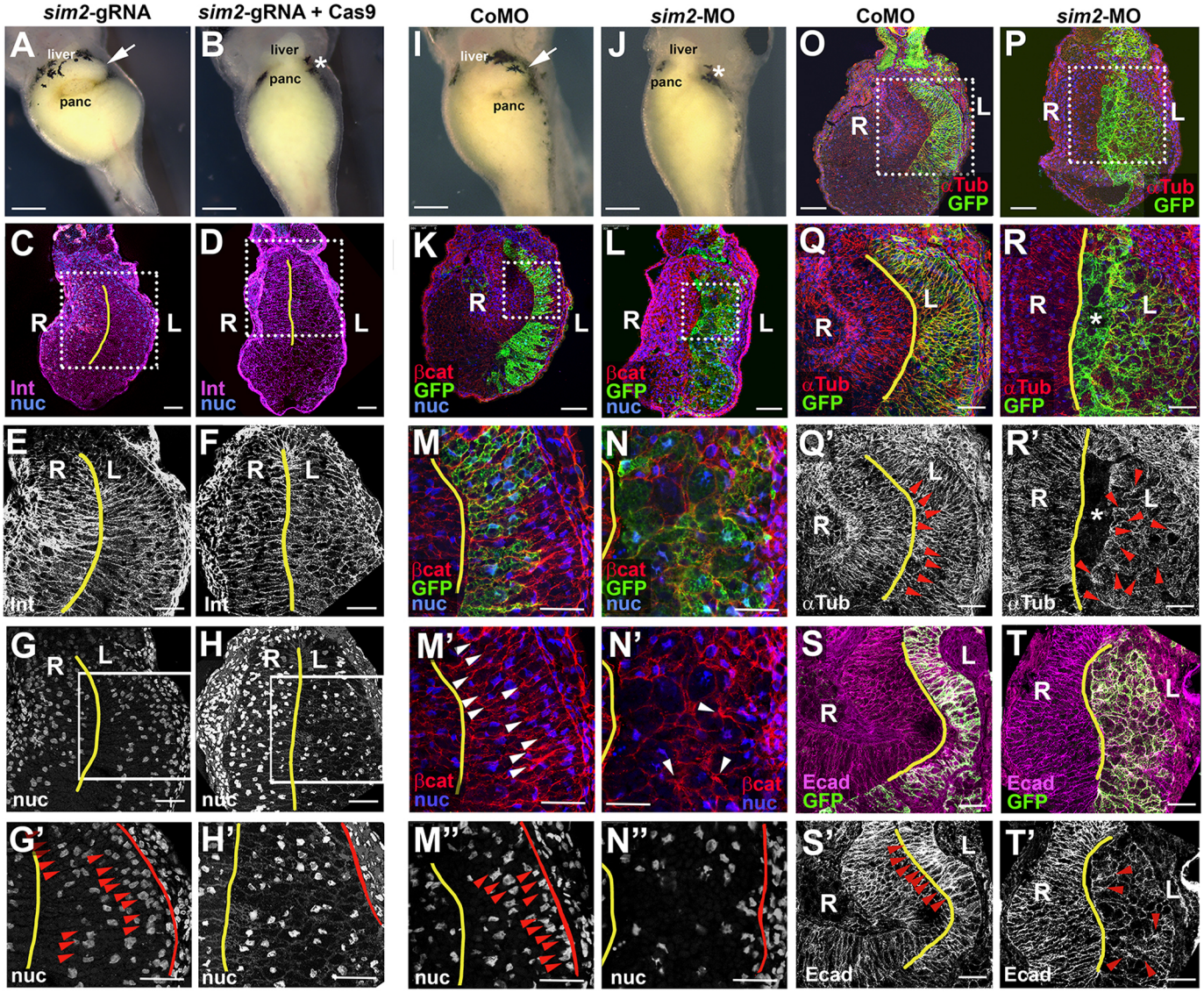

Fig. 3. *sim2* is required for cellular events underlying stomach curvature. (A-T′) *Xenopus* embryos were injected with *sim2* guide RNA alone (*sim2*-gRNA; A,C,E,G,G′), *sim2* gRNA plus Cas9 RNA (*sim2*-gRNA+Cas9; B,D,F,H,H′), control morpholino (CoMO; I,K,M-M″,O,Q,Q′,S,S′), *sim2* morpholino (*sim2*-MO; J,L,N-N″,P,R,R′,T,T′) and mRNA encoding GFP (K-T′). The greater curvature of the stomach (NF42) is indicated by arrows in control embryos (A,I; ventral views); asterisks indicate the absence of the greater curvature in Sim2 loss-of-function embryos (B,J). Sections through the stomach of *sim2*-gRNA or *sim2*-gRNA+Cas9 embryos (NF39) were stained to reveal Integrin (Int; magenta in C,D, white in E,F) and nuclei (nuc; blue in C,D, white in G-H′). The slit of the gut lumen dividing the right (R) and left (L) stomach walls is demarcated by yellow lines. The boxed areas in C, D, G and H are shown in magnified view in E and G, F and H, G′, and H′, respectively. In the left wall of control stomachs (G,G′), endoderm nuclei are aligned (red arrowheads, G′) and accumulating in close proximity to the basement membrane (BM, red line in G′). However, in the left wall of *sim2*-CRISPR stomachs (H,H′), endoderm nuclei remain broadly distributed between the apical surface (yellow line) and BM (red line). Sections through the stomach region of CoMO or *sim2*-MO embryos (NF39) were stained to reveal β-catenin (βcat, red; K-N′), α-tubulin (αTub, red in O-R, white in Q′,R′), E-cadherin (Ecad, magenta in S,T, white in S′,T′), GFP (green; K-N,O-R,S,T) and/or nuclei (nuc; blue in K-N′; white in M″,N″). The boxed areas in K, L, O and P are shown in magnified view in M-M″, N-N″, Q,Q′ (with a neighboring section shown in S,S') and R,R′ (with a neighboring section shown in T,T′), respectively. In the left wall of CoMO stomachs, endoderm cells are columnar (M,Q,S), with consistently basolaterally localized βcat (arrowheads, M′) and E-cad (arrowheads, S′), and apicobasally polarized microtubules (αTub; arrowheads, Q′). In contrast, endoderm cells in *sim2*-deficient stomachs are rounded (N,R,T), with irregular βcat (arrowheads, N′) and E-cad (arrowheads, T′) distribution, and sparse, randomly-oriented microtubules (arrowheads, R′). *sim2*-MO injected (GFP-positive) apoptotic cells, devoid of tubulin staining, are evident in the gut lumen (asterisks in R,R′). In the left wall of CoMO stomachs (M″), endoderm nuclei are radially aligned (arrowheads) and accumulating near the BM (red line). However, in the left wall of *sim2*-MO stomachs (N″), the nuclei of the disorganized endoderm layer remain broadly and randomly distributed. See Fig. S2 for *sim2* CRISPR-induced indels, Fig. S3 for *sim2* morpholino validation and Fig. S4 for additional characterization/validation of *sim2*-MO cellular phenotypes. Scale bars: 500 µm (A,B,I,J); 100 µm (C,D,K,L,O,P); 50 µm (E,F,G-H′,M-N″,Q-T′).

cell polarity and decreases E-cadherin, contributing to metastatic epithelial-mesenchymal transitions (EMT) in breast cancer (Micalizzi et al., 2010). In other cancers, *Sim2s* is upregulated, repressing the expression of differentiation genes (e.g. Aleman et al., 2005; DeYoung et al., 2003a; Halvorsen et al., 2007; Lu et al., 2011). The ability of single-minded genes to modulate epithelial plasticity in a context-dependent manner may be advantageous in the developing stomach wall, where cell rearrangement (i.e. tissue expansion) and differentiation (i.e. gastric epithelial maturation) must be dynamically balanced (Davis et al., 2017).

Development (2021) 148, dev199265. doi:10.1242/dev.199265

The effects of *sim2* deficiency are similar to those previously reported for loss of *pitx2* function (Davis et al., 2017). However, in contrast to Pitx2, Sim2 is insufficient to drive stomach curvature itself, i.e., overexpression of *sim2* on the right side has no effect on stomach morphology (Fig. S5), suggesting it may exert its effects only in the context of other bHLH/PAS dimerization partners or other cues also present only in the left stomach wall. It is notable that several potential direct targets of Sim2 (Letourneau et al., 2015) are LR asymmetrically expressed in the stomach. Interestingly, such molecules include vimentin, an intermediate filament protein involved in epithelial-mesenchymal plasticity, and Zic2, a zinc-finger molecule required for multiple earlier phases of LR asymmetry development (Dykes et al., 2018; Barratt et al., 2013).

In the fly, *sim* is expressed in the midline of both the CNS and gut tube and is a master regulator of midline development (Nambu et al., 1991), consistent with its association with pioneer factors and binding of super-enhancers (Letourneau et al., 2015). In vertebrates, *Sim2* is also expressed in the midline of the brain (Marion et al., 2005) and, as shown here, in the dorsal midline of the foregut. It is well known that midline structures (e.g. notochord) are crucial for the acquisition and maintenance of the LR body axis, acting as physical and/or chemical barriers to isolate the left versus right sides of the early embryo (e.g. Bisgrove et al., 2000; Danos and Yost, 1996; Przemeck et al., 2003). The expression of *sim2* in the midline of the foregut could serve a similar purpose within the stomach itself, segregating the distinct signaling and morphogenetic events occurring in the contralateral walls of a single organ.

In humans, *SIM2* maps within the Down syndrome (DS)-critical region of chromosome 21 (Shamblott et al., 2002). In mammalian embryos, *SIM2* is expressed in the brain and craniofacial structures affected in DS (Dahmane et al., 1995; Fan et al., 1996; Yamaki et al., 1996) and the triplication of *SIM2*, a transcriptional repressor (Moffett et al., 1997), may contribute to DS phenotypes (Chrast et al., 2000; Ema et al., 1999). *SIM2* is also expressed in the human embryo stomach (Rachidi et al., 2005), although whether it is left-sided is unknown, and whether single-minded genes are expressed asymmetrically in the mouse embryo has not yet been determined. Nonetheless, we note that individuals with DS exhibit an increased incidence of upper GI conditions also observed in patients with LR anomalies, such as gastric inlet/outlet obstructions (e.g. duodenal atresia, esophageal atresia; Benjamin et al., 1996; Cleves et al., 2007; Heinke et al., 2020; Stoll et al., 2015), annular pancreas, diaphragmatic hernia (Morris et al., 2014) and gastroesophageal reflux disease (GERD; Holmes, 2014; Macchini et al., 2011). Our discovery that a DS-related gene is expressed LR asymmetrically suggests the intriguing possibility that altered dosage (i.e. ectopic or overexpression) of LR genes may contribute to phenotypes seen in non-laterality-related birth defects.

MATERIALS AND METHODS

Animals and breeding

Animals were housed in the North Carolina State University College of Veterinary Medicine vivarium in accordance with Institutional Animal Care and Use Committee (IACUC) regulations. *Xenopus laevis in vitro* fertilization, embryo culture and staging (according to Nieuwkoop and Faber; Nieuwkoop and Faber, 1994) were performed according to established methods (Sive et al., 2000). *L. laevis* embryos were collected from natural matings as previously described (Amin et al., 2015) and were staged according to Gosner (Gosner, 1960). Embryos were raised at 23°C or 28°C and anesthetized according to standard procedure (Sive et al., 2000) before phenotyping or further processing for ISH and immunohistochemical analyses.

RNA sequencing

The left and right stomach walls of *L. laevis* were manually dissected from anesthetized embryos at GS18, GS19, GS20 and GS21 with sharpened forceps. At each stage, the anterior portion of the embryo (including the head, heart and pharyngeal region of the foregut) and the posterior portion of the embryo (immediately caudal to the liver) were removed and discarded, leaving only a transverse slice of tissue containing the stomach region of the foregut. The dorsal portion of the slice (containing the notochord, somites and pronephros) was discarded, leaving only the stomach, liver and ventral pancreas. The left and right halves of the stomach tube, i.e., the tissues on either side of the slit-like central lumen, surrounded by the outer epidermis, were then easily bisected and collected in Trizol (Ambion). Tissues from multiple embryos were pooled such that each replicate consisted of ten left or ten right half-stomachs; three pooled replicates were collected for each stage. The tissues were stored at −80°C until RNA isolation, which was accomplished by standard Trizol extraction followed by lithium chloride precipitation. Integrity and quantity of RNA yield was confirmed on a Thermo Fisher Scientific Nanodrop 1000 and an Agilent 2100 Bioanalyzer. RNA-seq was performed by Novogene with a poly-A selected non-stranded library prepared with NEBNext® Ultra™ RNA Library Prep Kit (New England BioLabs). An Illumina Novaseq 6000 was used for sequencing (PE150; Q30≥80%).

Bioinformatics

Raw reads were trimmed for quality and removal of sequencing adaptors (NEBNext® Ultra™ RNA Library Prep Kit) using Trimmomatic version 0.36 (Bolger et al., 2014). Trimmed, paired-end reads for each stage and replicate were independently aligned to the soft-masked *L. laevis* genome (provided by Austin Mudd and Daniel Rokhsar, University of California, Berkeley, USA) using HiSat2 version 2.1.0 (Kim et al., 2019a). The aligned reads were then sorted with samtools, and soft-clipping was removed with custom bash scripts (Li et al., 2009). Gene models were defined by cufflinks and merged into a single gene-transfer file (gtf format) with cuffmerge (Trapnell et al., 2012). A fasta file of the merged transcriptome was produced using gffread (Pertea and Pertea, 2020).

Differential expression analysis was performed by CuffDiff2 version 2.2.1 (Trapnell et al., 2013). The resulting files were then analyzed using the R package, cummeRbund version 2.30.0 (http://bioconductor.org/packages/devel/bioc/html/cummeRbund.html). Human gene symbols were assigned to the *L. laevis* genes using the top hit found by querying the *L. laevis* transcriptome with BLASTx against human protein sequences from Ensembl (Altschul et al., 1990; Zerbino et al., 2018).

Left or right-enriched genes were defined as having a log2 right/left ratio with a q-value ≤0.05 during at least one phase of stomach morphogenesis. Genes with no read counts in at least one sample were removed from further analysis; fifteen genes that reversed expression from significantly left-enriched to significantly right-enriched (or vice versa) during stomach morphogenesis were also excluded, as such expression patterns tended to be generated by outliers among the biological replicates. The R packages 'VennDiagram' and 'Heatmap2' were used to create figures (Chen, 2016; https://cran.r-project.org/web/packages/gplots/index.html) with only highly significant genes (q-value≤0.01).

In situ hybridization

Whole mount ISH was performed on *Xenopus* embryos as previously described (Dush and Nascone-Yoder, 2013). Embryos were fixed in MEMFA [100 mM MOPS (pH 7.4), 2 mM EGTA, 1 mM $MgSO_4$, 3.7% (v/v) formaldehyde] for 3 h, or 4% paraformaldehyde (PFA) overnight, at room temperature before being gradually dehydrated in methanol and stored at −20°C. Digoxigenin-labeled riboprobes were synthesized from linearized plasmids containing *X. laevis Sox2*, *Sim2* or *Pitx2* coding sequences using standard methodology (Sive et al., 2007).

ISH on tissue sections was performed as previously described (Butler et al., 2001) with the following modifications. Upon rehydration, sections were re-fixed with MEMFA for 30 min. After overnight probe hybridization, slides were washed with saline-sodium phosphate-EDTA, pH 7.4 (SSPE) before being treated with 20 µg/ml RNase A in 4× SSPE for 30 min at 37°C. Slides were blocked with 0.5% blocking reagent (Roche,

Development (2021) 148, dev199265. doi:10.1242/dev.199265

11096176001) in Buffer 1 (Butler et al., 2001) for 2 h at room temperature before incubating with anti-DIG-AP Fab fragments (Roche, 11093274910, 1:5000) overnight at 4°C. At the conclusion of the color reaction, slides were fixed for 15 min with 4% PFA before being washed with PBS plus 0.1% (v/v) Tween 20 (PBT), dehydrated to Xylene, mounted with Permount and cover-slipped.

Functional perturbations

Pharmacological dosing of *Xenopus* embryos with SB505124 (Sigma-Aldrich, S4696) was conducted as previously described (Davis et al., 2017). Briefly, SB505124 was diluted to 5 µM in *Xenopus* culture medium (0.1× MMR); an equal volume of DMSO (solvent) was used as control. Embryos were treated from stage NF19/20 through to collection stage.

Microinjection of loss-of-function reagents (i.e. gRNAs/Cas9 reagents and MO oligonucleotides; see Supplementary Materials and Methods, 'Morpholino sequences', for sequences) in *Xenopus* embryos was performed at the one-cell stage (300 pg gRNA), or at the eight-cell stage (8 ng MO), targeting a blastomere fated to contribute to the left or right side of the foregut, as previously described (Davis et al., 2017). *Cas9* mRNA and *sim2* gRNA were transcribed *in vitro* as previously described (Guo et al., 2014); *Cas9* mRNA was injected at 200 pg/nl. The MO-resistant version of *sim2* mRNA includes seven nucleotide changes that preserve the wild-type Sim2 amino acid sequence (see 'Morpholino-resistant *sim2* mRNA' in Supplementary Materials and Methods).

For gain-of-function studies, a dexamethasone-inducible synthetic mRNA encoding *Xenopus Pitx2c* (*Pitx2-GR*) was injected at the eight-cell stage, targeting a blastomere fated to contribute to the right side of the foregut, as previously described (Davis et al., 2017). *Pitx2*-GR mRNA injected embryos were subsequently exposed to dexamethasone (10 µM) or ethanol (solvent control) from stage 19/20. In all microinjection experiments, synthetic GFP and/or RFP mRNA, transcribed *in vitro* using the mMessage mMachine kit (Thermo Fisher Scientific), was co-injected as a lineage tracer to validate proper tissue targeting.

Immunohistochemistry

Immunohistochemistry was performed on transverse stomach sections of control and experimental *Xenopus* embryos, as previously described (Davis et al., 2017). Embryos were fixed by washing eight times with Dent's fixative (80% methanol/20% DMSO) before overnight storage at −20°C. Processing for cryosectioning was carried out as previously described (Dush and Nascone-Yoder, 2013). Slides were post-fixed with 4% PFA [100 mM Hepes (pH 7.4), 100 mM NaCl, 4% PFA] for 2 min, washed with PBT, and blocked for 1 h. Immunohistochemical staining was performed overnight at 4°C with blocking buffer containing primary antibodies (see Supplementary Materials and Methods, 'List of Antibodies', for the list of primary and secondary antibodies used). Sections were washed with PBT, stained with secondary antibodies as previously described (Davis et al., 2017; Dush and Nascone-Yoder, 2013), and slides were again washed with PBT and PBS before staining with Topro-3 (Thermo Fisher Scientific, T3604, 1:1000) in PBS for 5 min. Final slides were washed with PBS and mounted with Prolong Gold (Thermo Fisher Scientific), cured overnight in the dark, and visualized with a Leica DM 2500 confocal microscope.

Statistical analysis

Morphometric measurements of the width of the left and right stomach walls were performed using ImageJ software (National Institutes of Health). For ISH and immunohistochemistry data, multiple sections (anterior to posterior) of at least three different embryos were analyzed for each experimental condition. All perturbation experiments were performed at least in triplicate (total n=35-155 embryos per condition, with similar results across independent trials). Statistical significance was analyzed by one-way ANOVA with post-hoc Tukey HSD.

Acknowledgements

We are indebted to the North Carolina State University (NCSU) Genomic Sciences Laboratory, Betsy Scholl (NCSU Bioinformatics Consulting and Service Core) and Dereje Jima (NCSU Center for Human Health and the Environment) for bioinformatics consulting, Alex Dornburg (The University of North Carolina at Charlotte) for assistance with phylogenetics, and members of the Nascone-Yoder lab for helpful comments on the manuscript.

Competing interests

The authors declare no competing or financial interests.

Author contributions

Conceptualization: N.M.N.-Y.; Methodology: B.H.W., N.M.A., M.K.D., J.A.Y., N.M.N.-Y.; Formal analysis: B.H.W., N.M.A., D.W.; Investigation: B.H.W., N.M.A., K.B., D.W., M.K.D.; Resources: N.M.N.-Y.; Data curation: B.H.W.; Writing - original draft: N.M.A., N.M.N.-Y.; Writing - review & editing: B.H.W., D.W., M.K.D., N.M.N.-Y.; Visualization: N.M.A., D.W., J.A.Y., N.M.N.-Y.; Supervision: J.A.Y., N.M.N.-Y.; Funding acquisition: N.M.N.-Y.

Funding

Funding for this work was made possible through grants from the National Institutes of Health/Eunice Kennedy Shriver National Institute of Child Health and Human Development (R01 HD095937 to N.M.N.-Y.), and the National Institutes of Health/National Institute of Environmental Health Sciences (P30ES025128). Deposited in PMC for release after 12 months.

Data availability

Raw RNA-seq reads and the assembled transcriptome have been deposited in NCBI under the project accession number (PRJNA686137). Custom scripts used to perform the differential expression analysis and generate figures are available on GitHub (github.com/djwcisel/lep_lae_DEseq).

Peer review history

The peer review history is available online at https://journals.biologists.com/dev/article-lookup/doi/10.1242/dev.199265

References

Aleman, M. J., DeYoung, M. P., Tress, M., Keating, P., Perry, G. W. and Narayanan, R. (2005). Inhibition of Single Minded 2 gene expression mediates tumor-selective apoptosis and differentiation in human colon cancer cells. *Proc. Natl. Acad. Sci. USA* **102**, 12765-12770. doi:10.1073/pnas.0505484102

Altschul, S. F., Gish, W., Miller, W., Myers, E. W. and Lipman, D. J. (1990). Basic local alignment search tool. *J. Mol. Biol.* **215**, 403-410. doi:10.1016/S0022-2836(05)80360-2

Amin, N. M., Womble, M., Ledon-Rettig, C., Hull, M., Dickinson, A. and Nascone-Yoder, N. (2015). Budgett's frog (Lepidobatrachus laevis): A new amphibian embryo for developmental biology. *Dev. Biol.* **405**, 291-303. doi:10.1016/j.ydbio.2015.06.007

Barratt, K. S., Glanville-Jones, H. C. and Arkell, R. M. (2013). The Zic2 gene directs the formation and function of node cilia to control cardiac situs. *Genesis.* **52**, 626-635. doi:10.1002/dvg.22767

Benjamin, B., Jayakumar, P., Reddy, L. A. and Abbag, F. (1996). Gastric outlet obstruction caused by prepyloric web in a case of Down's syndrome. *J. Pediatr. Surg.* **31**, 1290-1291. doi:10.1016/S0022-3468(96)90254-7

Bisgrove, B. W., Essner, J. J. and Yost, H. J. (2000). Multiple pathways in the midline regulate concordant brain, heart and gut left-right asymmetry. *Development* **127**, 3567-3579. doi:10.1242/dev.127.16.3567

Bolger, A. M., Lohse, M. and Usadel, B. (2014). Trimmomatic: a flexible trimmer for Illumina sequence data. *Bioinformatics* **30**, 2114-2120. doi:10.1093/bioinformatics/btu170

Bossing, T. and Technau, G. M. (1994). The fate of the CNS midline progenitors in Drosophila as revealed by a new method for single cell labelling. *Development* **120**, 1895-1906. doi:10.1242/dev.120.7.1895

Butler, K., Zorn, A. M. and Gurdon, J. B. (2001). Nonradioactive in situ hybridization to xenopus tissue sections. *Methods* **23**, 303-312. doi:10.1006/meth.2000.1142

Chen, H. (2016). VennDiagram: Generate high-resolution Venn and Euler plots. *R package version* **1**, 1.

Chen, K.-J., Lizaso, A. and Lee, Y.-H. (2014). SIM2 maintains innate host defense of the small intestine. *Am. J. Physiol. Gastrointest. Liver Physiol.* **307**, G1044-G1056. doi:10.1152/ajpgi.00241.2014

Chrast, R., Scott, H. S., Madani, R., Huber, L., Wolfer, D. P., Prinz, M., Aguzzi, A., Lipp, H.-P. and Antonarakis, S. E. (2000). Mice trisomic for a bacterial artificial chromosome with the single-minded 2 gene (Sim2) show phenotypes similar to some of those present in the partial trisomy 16 mouse models of Down syndrome. *Hum. Mol. Genet.* **9**, 1853-1864. doi:10.1093/hmg/9.12.1853

Cleves, M. A., Hobbs, C. A., Cleves, P. A., Tilford, J. M., Bird, T. M. and Robbins, J. M. (2007). Congenital defects among liveborn infants with Down syndrome. *Birth Defects Research (Part A)* **79**, 657-663. doi:10.1002/bdra.20393

Dahmane, N., Charron, G., Lopes, C., Yaspo, M. L., Maunoury, C., Decorte, L., Sinet, P. M., Bloch, B. and Delabar, J. M. (1995). Down syndrome-critical region contains a gene homologous to Drosophila sim expressed during rat and human

central nervous system development. *Proc. Natl. Acad. Sci. USA* **92**, 9191-9195. doi:10.1073/pnas.92.20.9191

Danos, M. C. and Yost, H. J. (1996). Role of notochord in specification of cardiac left-right orientation in zebrafish and Xenopus. *Dev. Biol.* **177**, 96-103. doi:10.1006/dbio.1996.0148

Davis, A., Amin, N. M., Johnson, C., Bagley, K., Troy Ghashghaei, H. and Nascone-Yoder, N. (2017). Stomach curvature is generated by left-right asymmetric gut morphogenesis. *Development* **144**, 1477-1483. doi:10.1242/dev.143701

DeYoung, M. P., Tress, M. and Narayanan, R. (2003a). Identification of Down's syndrome critical locus gene SIM2-s as a drug therapy target for solid tumors. *Proc. Natl. Acad. Sci. USA* **100**, 4760-4765. doi:10.1073/pnas.0831000100

Dush, M. K. and Nascone-Yoder, N. M. (2013). Jun N-terminal kinase maintains tissue integrity during cell rearrangement in the gut. *Development* **140**, 1457-1466. doi:10.1242/dev.086850

Dush, M. K., McIver, A. L., Parr, M. A., Young, D. D., Fisher, J., Newman, D. R., Sannes, P. L., Hauck, M. L., Deiters, A. and Nascone-Yoder, N. (2011). Heterotaxin: a TGF-β signaling inhibitor identified in a multi-phenotype profiling screen in Xenopus embryos. *Chem. Biol.* **18**, 252-263. doi:10.1016/j.chembiol.2010.12.008

Dykes, I. M., Szumska, D., Kuncheria, L., Puliyadi, R., Chen, C.-M., Papanayotou, C., Lockstone, H., Dubourg, C., David, C., Schneider, J. E. et al. (2018). A requirement for Zic2 in the regulation of nodal expression underlies the establishment of left-sided identity. *Sci. Rep.* **8**, 10439. doi:10.1038/s41598-018-28714-1

Ema, M., Ikegami, S., Hosoya, T., Mimura, J., Ohtani, H., Nakao, K., Inokuchi, K., Katsuki, M. and Fujii-Kuriyama, Y. (1999). Mild impairment of learning and memory in mice overexpressing the mSim2 gene located on chromosome 16: an animal model of Down's syndrome. *Hum. Mol. Genet.* **8**, 1409-1415. doi:10.1093/hmg/8.8.1409

Fan, C.-M., Kuwana, E., Bulfone, A., Fletcher, C. F., Copeland, N. G., Jenkins, N. A., Crews, S., Martinez, S., Puelles, L., Rubenstein, J. L. R. et al. (1996). Expression patterns of two murine homologs of Drosophila single-minded suggest possible roles in embryonic patterning and in the pathogenesis of Down syndrome. *Mol. Cell. Neurosci.* **7**, 1-16. doi:10.1006/mcne.1996.0001

Gosner, K. L. (1960). A simplified table for staging anuran embryos and larvae with notes on identification. *Herpetologica* **16**, 183-190.

Grimes, D. T. and Burdine, R. D. (2017). Left-right patterning: breaking symmetry to asymmetric morphogenesis. *Trends Genet.* **33**, 616-628. doi:10.1016/j.tig.2017.06.004

Grzymkowski, J., Wyatt, B. and Nascone-Yoder, N. (2020). The twists and turns of left-right asymmetric gut morphogenesis. *Development* **147**, dev187583. doi:10.1242/dev.187583

Guo, X., Zhang, T., Hu, Z., Zhang, Y., Shi, Z., Wang, Q., Cui, Y., Wang, F., Zhao, H. and Chen, Y. (2014). Efficient RNA/Cas9-mediated genome editing in Xenopus tropicalis. *Development* **141**, 707-714. doi:10.1242/dev.099853

Halvorsen, O. J., Rostad, K., Øyan, A. M., Puntervoll, H., Bø, T. H., Stordrange, L., Olsen, S., Haukaas, S. A., Hood, L., Jonassen, I. et al. (2007). Increased expression of SIM2-s protein is a novel marker of aggressive prostate cancer. *Clin. Cancer Res.* **13**, 892-897. doi:10.1158/1078-0432.CCR-06-1207

Heinke, D., Isenburg, J. L., Stallings, E. B., Short, T. D., Le, M., Fisher, S., Shan, X., Kirby, R. S., Nguyen, H. H., Nestoridi, E. et al. (2020). Prevalence of structural birth defects among infants with Down Syndrome, 2013-2017: a US population-based study. *Birth Defects Research* **113**, 189-202. doi:10.1002/bdr2.1854

Holmes, G. (2014). Gastrointestinal disorders in Down syndrome. *Gastroenterol Hepatol Bed Bench* **7**, 6-8.

Kim, D., Paggi, J. M., Park, C., Bennett, C. and Salzberg, S. L. (2019a). Graph-based genome alignment and genotyping with HISAT2 and HISAT-genotype. *Nat. Biotechnol.* **37**, 907-915. doi:10.1038/s41587-019-0201-4

Kim, W. K., Kwon, Y., Jang, M., Park, M., Kim, J., Cho, S., Jang, D. G., Lee, W.-B., Jung, S. H., Choi, H. J. et al. (2019b). β-catenin activation down-regulates cell-cell junction-related genes and induces epithelial-to-mesenchymal transition in colorectal cancers. *Sci. Rep.* **9**, 18440. doi:10.1038/s41598-019-54890-9

Laffin, B., Wellberg, E., Kwak, H.-I., Burghardt, R. C., Metz, R. P., Gustafson, T., Schedin, P. and Porter, W. W. (2008). Loss of singleminded-2s in the mouse mammary gland induces an epithelial-mesenchymal transition associated with up-regulation of slug and matrix metalloprotease 2. *Mol. Cell. Biol.* **28**, 1936-1946. doi:10.1128/MCB.01701-07

Letourneau, A., Cobellis, G., Fort, A., Santoni, F., Garieri, M., Falconnet, E., Ribaux, P., Vannier, A., Guipponi, M., Carninci, P. et al. (2015). HSA21 Single-Minded 2 (Sim2) binding sites co-localize with super-enhancers and pioneer transcription factors in pluripotent mouse ES cells. *PLoS ONE* **10**, e0126475. doi:10.1371/journal.pone.0126475

Li, H., Handsaker, B., Wysoker, A., Fennell, T., Ruan, J., Homer, N., Marth, G., Abecasis, G., Durbin, R. and **1000 Genome Project Data Processing Subgroup**. (2009). The Sequence Alignment/Map format and SAMtools. *Bioinformatics* **25**, 2078-2079. doi:10.1093/bioinformatics/btp352

Lu, B., Asara, J. M., Sanda, M. G. and Arredouani, M. S. (2011). The role of the transcription factor SIM2 in prostate cancer. *PLoS ONE* **6**, e28837. doi:10.1371/journal.pone.0028837

Macchini, F., Leva, E., Torricelli, M. and Valadè, A. (2011). Treating acid reflux disease in patients with Down syndrome: pharmacological and physiological approaches. *Clin. Exp. Gastroenterol.* **4**, 19-22. doi:10.2147/CEG.S15872

Maeda, R., Hozumi, S., Taniguchi, K., Sasamura, T., Murakami, R. and Matsuno, K. (2007). Roles of single-minded in the left-right asymmetric development of the Drosophila embryonic gut. *Mech. Dev.* **124**, 204-217. doi:10.1016/j.mod.2006.12.001

Marion, J.-F., Yang, C., Caqueret, A., Boucher, F. and Michaud, J. L. (2005). Sim1 and Sim2 are required for the correct targeting of mammillary body axons. *Development* **132**, 5527-5537. doi:10.1242/dev.02142

Micalizzi, D. S., Farabaugh, S. M. and Ford, H. L. (2010). Epithelial-mesenchymal transition in cancer: parallels between normal development and tumor progression. *J. Mammary Gland Biol. Neoplasia* **15**, 117-134. doi:10.1007/s10911-010-9178-9

Moffett, P., Reece, M. and Pelletier, J. (1997). The murine Sim-2 gene product inhibits transcription by active repression and functional interference. *Mol. Cell. Biol.* **17**, 4933-4947. doi:10.1128/MCB.17.9.4933

Morris, J. K., Garne, E., Wellesley, D., Addor, M., Arriola, L., Barisic, I., Beres, J., Bianchi, F., Budd, J., Dias, C. M. et al. (2014). Major congenital anomalies in babies born with Down syndrome: a EUROCAT population-based registry study. *Am. J. Med. Genet. A* **164**, 2979-2986. doi:10.1002/ajmg.a.36780

Nambu, J. R., Lewis, J. O., Wharton, K. A., Jr and Crews, S. T. (1991). The Drosophila single-minded gene encodes a helix-loop-helix protein that acts as a master regulator of CNS midline development. *Cell* **67**, 1157-1167. doi:10.1016/0092-8674(91)90292-7

Nieuwkoop, P. and Faber, J. (1994). *Normal Table of Xenopus laevis (Daudin)*. New York & London: Garland Publishing Inc.

Pertea, G. and Pertea, M. (2020). GFF Utilities: GffRead and GffCompare. *F1000Res.* **9**, 304. doi:10.12688/f1000research.23297.1

Przemeck, G. K. H., Heinzmann, U., Beckers, J. and Hrabé de Angelis, M. (2003). Node and midline defects are associated with left-right development in Delta1 mutant embryos. *Development* **130**, 3-13. doi:10.1242/dev.00176

Rachidi, M., Lopes, C., Charron, G., Delezoide, A.-L., Paly, E., Bloch, B. and Delabar, J.-M. (2005). Spatial and temporal localization during embryonic and fetal human development of the transcription factor SIM2 in brain regions altered in Down syndrome. *Int. J. Dev. Neurosci.* **23**, 475-484. doi:10.1016/j.ijdevneu.2005.05.004

Shamblott, M. J., Bugg, E. M., Lawler, A. M. and Gearhart, J. D. (2002). Craniofacial abnormalities resulting from targeted disruption of the murine Sim2 gene. *Dev. Dyn.* **224**, 373-380. doi:10.1002/dvdy.10116

Sive, H. L., Grainger, R. M. and Harland, R. M. (2000). *Early development of Xenopus laevis: A Laboratory Manual*. CSHL Press.

Sive, H. L., Grainger, R. M. and Harland, R. M. (2007) Synthesis and purification of digoxigenin-labeled RNA probes for in situ hybridization. *CSH Protoc.* **2007**, pdb.prot4778. doi:10.1101/pdb.prot4778

Stoll, C., Dott, B., Alembik, Y. and Roth, M.-P. (2015). Associated congenital anomalies among cases with Down syndrome. *Eur. J. Med. Genet.* **58**, 674-680. doi:10.1016/j.ejmg.2015.11.003

Thomas, J. B., Crews, S. T. and Goodman, C. S. (1988). Molecular genetics of the single-minded locus: a gene involved in the development of the Drosophila nervous system. *Cell* **52**, 133-141. doi:10.1016/0092-8674(88)90537-5

Trapnell, C., Roberts, A., Goff, L., Pertea, G., Kim, D., Kelley, D. R., Pimentel, H., Salzberg, S. L., Rinn, J. L. and Pachter, L. (2012). Differential gene and transcript expression analysis of RNA-seq experiments with TopHat and Cufflinks. *Nat. Protoc.* **7**, 562-578. doi:10.1038/nprot.2012.016

Trapnell, C., Hendrickson, D. G., Sauvageau, M., Goff, L., Rinn, J. L. and Pachter, L. (2013). Differential analysis of gene regulation at transcript resolution with RNA-seq. *Nat. Biotechnol.* **31**, 46-53. doi:10.1038/nbt.2450

Yamaki, A., Noda, S., Kudoh, J., Shindoh, N., Maeda, H., Minoshima, S., Kawasaki, K., Shimizu, Y. and Shimizu, N. (1996). The mammalian single-minded (SIM) gene: mouse cDNA structure and diencephalic expression indicate a candidate gene for Down syndrome. *Genomics* **35**, 136-143. doi:10.1006/geno.1996.0332

Zerbino, D. R., Achuthan, P., Akanni, W., Amode, M. R., Barrell, D., Bhai, J., Billis, K., Cummins, C., Gall, A., Girón, C. G. et al. (2018). Ensembl 2018. *Nucleic Acids Res.* **46**, D754-D761. doi:10.1093/nar/gkx1098